Supplementary Information

Enhanced Efficiency of Polymer Photovoltaic Cells via the Incorporation of a Water Soluble Naphthalene Diimide Derivative as Cathode Interlayer

Kang Zhao,[a,b] Long Ye,[b,*] Wenchao Zhao,[a] Shaoqing Zhang,[b] Huifeng Yao,[b] Bowei Xu,[b] Mingliang Sun,[a,*] and Jianhui Hou[b,*]

[a] Institute of Material Science and Engineering, Ocean University of China, Qingdao 266100, P. R. China

[b] State Key Laboratory of Polymer Physics and Chemistry, Beijing National Laboratory for Molecular Sciences, Institute of Chemistry, Chinese Academy of Sciences, Beijing 100190, P. R. China

*Corresponding authors:

mlsun@ouc.edu.cn (Dr. M. Sun); yelong@iccas.ac.cn (Dr. L. Ye); hjhzlz@iccas.ac.cn (Prof. J. Hou), Tel: +86-10-82615900.
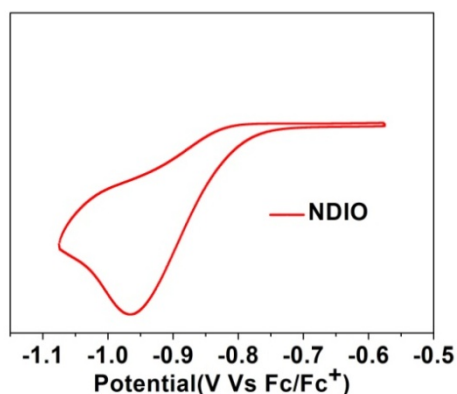
S1. TGA plot of NDIO
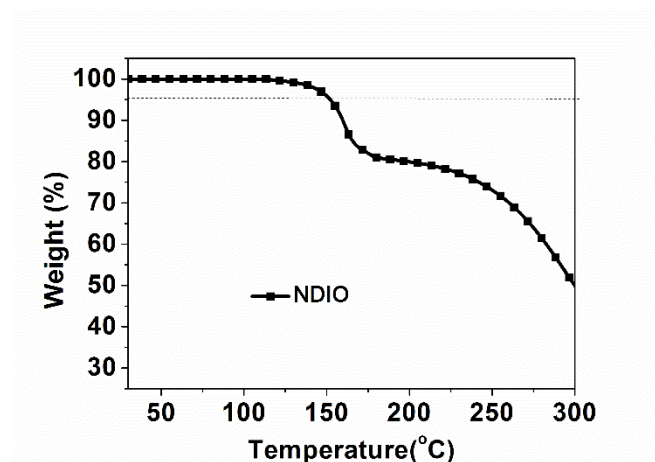
Fig. S1. TGA curve of NDIO.

As shown in Fig. S1, the weight of NDIO sample will decrease from ~160 °C.
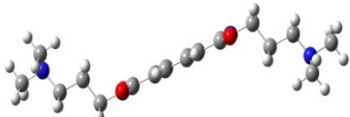
S2. Cyclic voltammetry curve of NDIO

**Fig. S2**. The cyclic voltammetry curve of NDIO in Bu_4NPF_6/methanol(0.1 M) solution.

A glassy carbon electrode was used as the working electrode, whereas a platinum wire was employed as the counter electrode and Ag/AgCl served as the reference electrode. CV measurements were carried out in Bu_4NPF_6/methanol (0.1M) solution at ambient temperature under a nitrogen atmosphere at a scan rate of 50 mV/s.

S3. Density Functional Theory (DFT) calculation

Table S1. Density Functional Theory (DFT) calculation for dipole moment of NDI (compound 2 in Fig. 1a) and NDIO molecules.

| compound	Optimized geometry	Dipole moment
NDI		0.7389
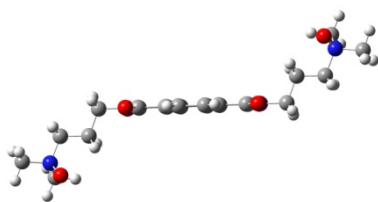
NDIO   5.8649

Density Functional Theory (DFT) at B3YLP/6-31G(d,p) level was utilized to calculate the dipole moment of NDI and amino N-oxide NDIO molecules. The results exhibit that amino N-oxide derivatives can provide larger dipole moment than the amine group does. Therefore, the different dipole moment could be expected to explain the difference of work function tuning once the NDI or NDIO was spin-coated on the top of pristine ITO (the detailed data was not listed here).

S4. Photovoltaic performance of PBDT-TS1/PC$_{71}$BM-based Inverted PPC device with NDIO processed by methanol.

Table S2. Photovoltaic parameters of PBDT-TS1/PC$_{71}$BM-based inverted PPC device with NDIO processed by methanol.

|	V_{oc}	J_{sc}	FF	PCE
Inverted device	[V]	[mA/cm^2]	[%]	[%]
NDIO in methanol	0.777	18.61	67.40	9.74
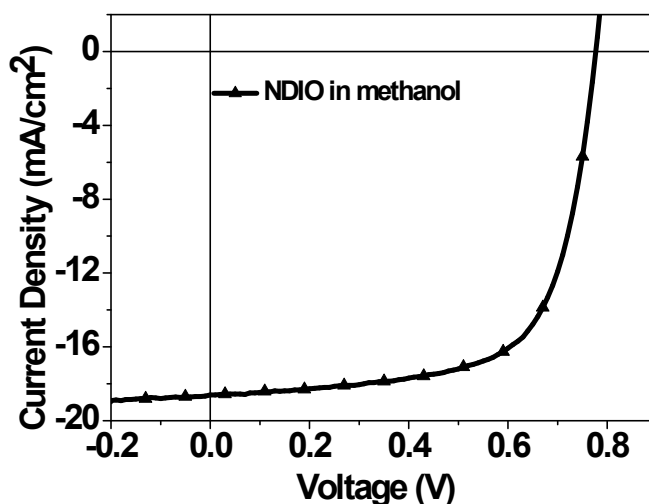
Fig. S3. Typical *J-V* curve of PBDT-TS1/PC$_{71}$BM-based inverted PPC device with NDIO processed by methanol.

S5. Photovoltaic performances of PBDT-TS1/PC$_{71}$BM-based inverted PPC devices with PEIE and ZnO cathode interlayers.

Table S3. Photovoltaic parameters of PBDT-TS1/PC$_{71}$BM-based inverted PPC devices with PEIE and ZnO cathode interlayers.

Inverted device	V_{oc} [V]	J_{sc} [mA/cm^2]	FF [%]	PCE [%]
ZnO	0.784	18.11	68.10	9.67
PEIE	0.777	17.94	66.83	9.32
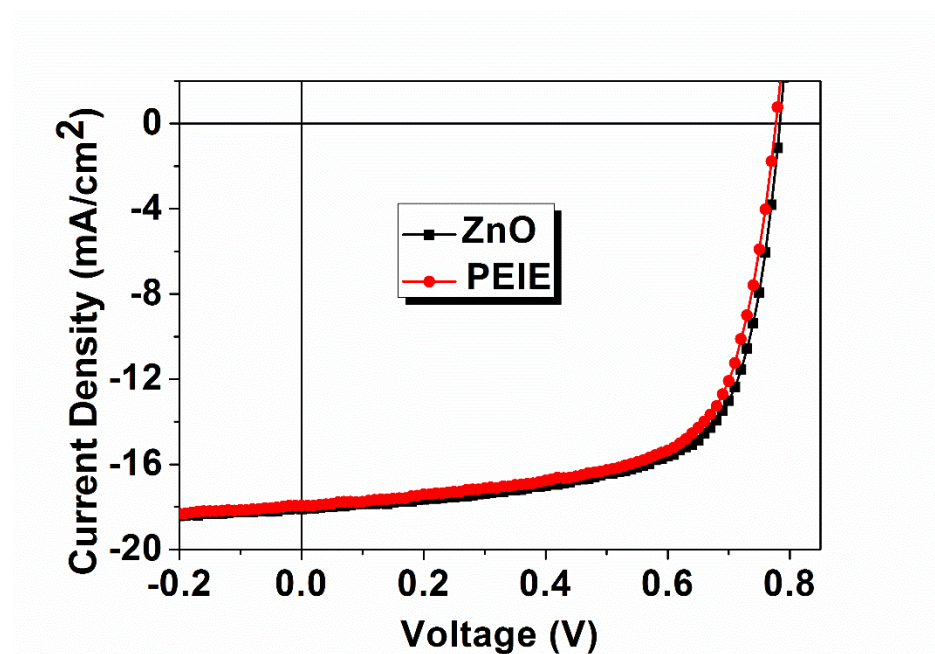
Fig. S4. Typical *J-V* curves of PBDT-TS1/PC$_{71}$BM-based inverted PPC devices with PEIE and ZnO cathode interlayers.

S6. Device PCEs of PBDT-TS1/PC$_{71}$BM-based PPC devices with NDIO cathode layers casted from different concentrations.
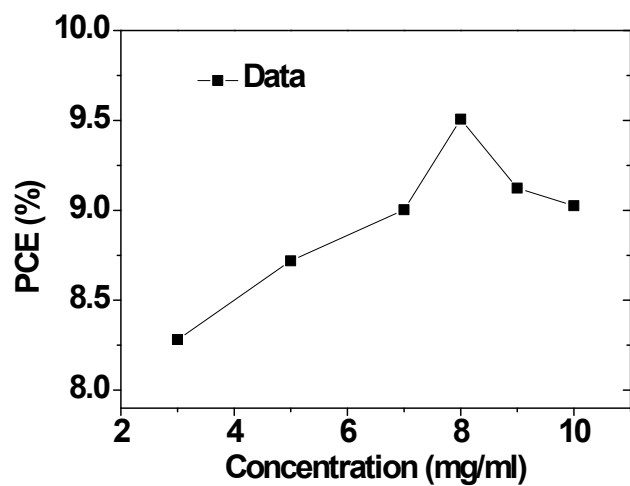
Fig. S5. PCE vs concentration plots of PBDT-TS1/PC$_{71}$BM-based PPC devices with NDIO cathode layers.